Extracting phase-dependent human vestibular reflexes during locomotion using both time and frequency correlation approaches

Jean-Sébastien Blouin, Christopher J. Dakin, Kees van den Doel, Romeo Chua, Bradford J. McFadyen and John Timothy Inglis

J Appl Physiol 111:1484-1490, 2011. First published 25 August 2011;
doi:10.1152/japplphysiol.00621.2011

J Appl Physiol 111: 1484–1490, 2011.
First published August 25, 2011; doi:10.1152/japplphysiol.00621.2011.

Extracting phase-dependent human vestibular reflexes during locomotion using both time and frequency correlation approaches

Jean-Sébastien Blouin,[1,2,3] Christopher J. Dakin,[1] Kees van den Doel,[3] Romeo Chua,[1] Bradford J. McFadyen,[5,6] and John Timothy Inglis[1,2,4]

[1]*School of Kinesiology,* [2]*Brain Research Center,* [3]*Institute for Computing, Information and Cognitive Systems, and* [4]*International Collaboration for Repair Discoveries, University of British Columbia, Vancouver, British Columbia;* [5]*Centre for Interdisciplinary Research in Rehabilitation and Social integration, and* [6]*Department of Rehabilitation, Laval University, Québec, Canada*

Submitted 17 May 2011; accepted in final form 22 August 2011

Blouin JS, Dakin CJ, van den Doel K, Chua R, McFadyen BJ, Inglis JT. Extracting phase-dependent human vestibular reflexes during locomotion using both time and frequency correlation approaches. *J Appl Physiol* 111: 1484–1490, 2011. First published August 25, 2011; doi:10.1152/japplphysiol.00621.2011.—Daily activities, such as walking, may require dynamic modulation of vestibular input onto motoneurons. This dynamic modulation is difficult to identify in humans due to limitations in the delivery and analysis of current vestibular probes, such as galvanic vestibular stimulation. Stochastic vestibular stimulation, however, provides an alternative method to extract human vestibular reflexes. Here, we used time-dependent coherence and time-dependent cross-correlation, coupled with stochastic vestibular stimulation, to investigate the phase dependency of human vestibular reflexes during locomotion. We found that phase-dependent activity from the medial gastrocnemius muscles is correlated with the vestibular signals over the 2- to 20-Hz bandwidth during the stance phase of locomotion. Vestibular-gastrocnemius coherence and time-dependent cross-correlations reached maximums at 21 ± 4 and 23 ± 8% of the step cycle following heel contact and before the period of maximal electromyographic activity (38 ± 5%). These results demonstrate *1*) the effectiveness of these techniques in extracting the phase-dependent modulation of vestibulomuscular coupling during a cyclic task; *2*) that vestibulomuscular coupling is phasically modulated during locomotion; and *3*) that the period of strongest vestibulomuscular coupling does not correspond to the period of maximal electromyographic activity in the gastrocnemius. Therefore, we have shown that stochastic vestibular stimulation, coupled with time-frequency decomposition, provides an effective tool to assess the contribution of vestibular ex-afference to the muscular control during locomotion.

stochastic vestibular stimulation; wavelet; time-dependent cross-correlation; electromyography

THE EVOLUTION OF LOCOMOTION from a multipedal to a bipedal task has resulted in a locomotor pattern with increased postural demand. Compared with quadrupeds, humans have a high center of mass perched over a small base of support, resulting in a generally unstable vertical posture. The inherent passive instability generated by this unstable vertical posture poses a challenge for human locomotor activity, because the alternating flexor-extensor muscle activity, which propels the body forwards, requires the active maintenance of upright balance to be successful (25). In humans, sensory systems, such as the vestibular system, aid in actively maintaining a vertical posture. During locomotion, however, the contribution of these systems becomes less clear. The vestibular system, for instance, has been inferred to contribute to locomotion through the changes in gait trajectory observed both in patients with unilateral vestibular neurotomy (3) or acute unilateral vestibular failure (4), and in participants receiving electric vestibular stimulation (2, 13, 15). In fact, most studies have been limited to describing the global effects of vestibular afference on locomotor control (2, 13, 15). In felines, in contrast, vestibular signals are modulated in phase with the locomotor step cycle and are believed to modulate extensor muscle tone (22, 23, 27). Similar modulation has been inferred in humans (1), but has only been directly documented once (17).

Our limited knowledge of the vestibular system's role in locomotion is partly due to the difficulty in probing and resolving vestibular reflexes during human locomotion. Typically, galvanic vestibular stimulation (GVS) is used to generate a vestibular ex-afferent-like signal, which results in biphasic responses in lower limb muscles actively involved in balance control (6, 14, 18, 26). The evoked muscular responses are small, requiring the averaging of many responses to clearly identify the vestibular reflex. Thus identifying these small biphasic vestibulomotor responses from the on-going locomotor activity can prove challenging (17). Indeed, Iles et al. (17) observed phase-dependent modulation of human vestibular reflexes, but had difficulty in resolving both the time course of modulation and the amplitude of the short-latency muscle response component. To overcome these limitations, we propose to use stochastic vestibular stimulation (SVS), in combination with time-frequency and time-dependent cross-correlation analysis techniques, to extract these time-varying vestibular reflexes. SVS is an alternative method to GVS, which has been shown to elicit similar vestibular responses to GVS delivered during human standing balance, but with reduced testing times and decreased postural disturbance (8–10). Compared with GVS, the continuous nature of the stochastic stimulus allows for the use of time-dependent decompositions that may help extract phasically modulated vestibular reflexes during cyclic activities, such as human locomotion. Here, we propose to develop a framework to assess phasic modulation of vestibulomotor responses in humans using SVS. Our primary aim is to characterize modulation of human vestibular reflexes across the locomotor step cycle using time-dependent correlations across both the time and frequency domains. In the time domain, time-dependent cross-correlations will be used to describe the shape and polarity of the evoked responses, whereas, in the frequency domain, time-dependent correlations

Address for reprint requests and other correspondence: J.-S. Blouin, 210-6081 Univ. Blvd., Vancouver, BC, V6T1Z1 Canada (e-mail: jsblouin@interchange.ubc.ca).

(coherence) will also be used to identify the time period and frequencies over which the SVS stimulus interacts with lower limb muscle activity. We hypothesized that vestibular reflexes will undergo phasic modulation during the gait cycle, exhibiting their largest responses during the stance phase, when ankle extensor tone should be at its maximum.

METHODS

Subjects. Nine healthy subjects (4 women, height 170 ± 9 cm, mass 68 ± 13 kg) between the ages of 21 and 34 yr, with no known history of neurological disease or injury, participated in this study. Each subject gave his or her written, informed consent to the procedures approved by the University of British Columbia's clinical research ethics board.

Stimulus. Binaural bipolar vestibular stimulation was delivered using gel-coated carbon rubber electrodes (9 cm^2) secured over the mastoid processes with an elastic headband. Bandwidth-limited stochastic vestibular signals (0–25 Hz; amplitude peak ± 4.5 mA, root mean square 1.05 mA), lasting 305 s, were created using Labview 8.5 software (National Instruments) and delivered using a constant-current stimulus isolation unit (model 2200, AM Systems).

Protocol. Participants walked on a treadmill at a speed of 0.4 m/s while maintaining a cadence of 52 steps/min (guided by a metronome) with their eyes open. This treadmill speed was chosen to replicate the speed used by Iles et al. (17) in their initial demonstration of phase-dependent vestibulomuscle responses during human locomotion where the cadence was matched to that used in previous locomotor studies using electrical vestibular stimulation (13, 15). Subjects maintained their Frankfurt plane 18° nose up relative to the floor by keeping a headgear-mounted laser on a target located on a wall 2 m ahead of them (7, 11, 14). These locomotor parameters and head positions were chosen to maximize the amplitude of the vestibular responses to mediolateral perturbations (13, 17). Volunteers walked while receiving SVS for three trials of 5 min. Rest periods were provided between trials at the request of the participant to avoid any signs of fatigue. Across trials, a minimum of 380 strides were performed for each individual.

Electromyography and signal analysis. Surface electromyography (EMG) was collected bilaterally from the medial head of gastrocnemius using self-adhesive Ag-AgCl surface electrodes (Ambu Blue Sensor M). The medial gastrocnemius was chosen because it exhibits large responses to mediolateral vestibular perturbations during locomotion (17). Foot switches were placed bilaterally under the surface of the shoe, near the heel and first toe regions, to estimate bilateral heel strike and toe off during locomotion. EMG was amplified (×5,000), band-pass filtered from 30 to 1,000 Hz (Neurolog NL-844, Digitimer), digitized along with the vestibular and foot switches signals at 2 kHz (PXI-6289, National Instruments), and saved on a personal computer for subsequent offline analyses.

Time and frequency correlations between the SVS and EMG signals were performed to estimate the averaged SVS-evoked muscular responses during locomotion (9, 10). Briefly, data from the three individual walking trials were pooled for each subject, yielding a total of 447 disjoint sections to perform the analysis (frequency resolution of 0.48 Hz). Pooled EMG data were full-wave rectified and then the auto- and cross-spectra for the SVS and muscle activity signals were computed for the bilateral gastrocnemius muscles. Frequency domain coherence between the SVS signal and EMG were estimated using a Matlab script for each trial condition within each participant to estimate the linear relationship between the two processes across various frequencies (16, 28).

Cross-correlations between the stochastic vestibular signal and the recorded muscle EMG were determined using the inverse Fourier transform of the cross-spectral estimate (5, 28) and were normalized by the norm of the input vectors to obtain unitless correlation values between −1 and +1 (10). Confidence intervals (with positive and negative 95% confidence limits) were computed to determine significant values on a subject-by-subject basis. Given our convention for positive vestibular signals corresponding to anode right (cathode left) currents, a positive correlation indicates that anode right (cathode left) currents induced a facilitation of muscle activity. Polarity, peak amplitude, and peak latency of the SVS-evoked responses were estimated using cross-correlations. Cross-correlations and coherence were averaged between subjects to represent the global response from all subjects.

To identify phasic modulations in the correlation between the vestibular stimulus and muscle activity during the locomotor cycle, coherence, gain, and cross-correlations between the SVS and EMG signals were computed as a function of time (using time-dependent coherence, gain, and time-dependent cross-correlations, respectively). Due to the nonstationarity of the EMG signals during walking, continuous wavelet decompositions of the signals were performed using the Morlet wavelet transform to estimate the time-dependent coherence (33). The SVS and EMG signals were preprocessed before estimating the coherence and cross-correlation over time. First, the signals were cut into strides synchronized on the right heel strike (determined from right heel foot switch contact signal). To avoid distortion in the correlations over time at either end of the signals (e.g., around right heel strike), the strides were padded with data from the previous (50%) and subsequent (50%) strides. EMG signals were full-wave rectified, and then both EMG and SVS signals were low-pass filtered (100 Hz cutoff, fourth-order dual-pass Butterworth filter) and resampled at 200 Hz.

The time-dependent coherence and gain were estimated using a modified procedure based on the method by Zhan et al. (33). Time-dependent cross-correlations were estimated using a custom-written algorithm, which is available as a Matlab freeware at http://www.cs.ubc.ca/~kvdoel/publications/tc.zip. To account for the variability of stride duration during locomotion, we normalized stride duration in time, for the time-dependent cross-correlation, gain and coherence, by resampling with respect to the average stride duration across trials. This time normalization was performed on the wavelet spectra for both the SVS and EMG signals, as well as their cross-spectrum, before estimating time-dependent coherence and gain.

Time normalization of stride duration was defined as

$$T = \sum_{i=1}^{N} T_i/N \tag{1}$$

where T is the average stride duration, i is the stride number, N is the total number of strides (380), and T_i is the stride duration for the ith stride. For each stride, the scaled stride time τ was defined as $\tau = tT/T_i$, which satisfies $0 \le \tau \le T$. Following stride normalization, the time-dependent cross-correlation $C(\tau, \lambda)$ (λ is the lag time), between x and y as a function of scaled time was determined through the use of the follow equation:

$$C(\tau,\lambda) = \frac{\sum_{i=1}^{N} \tilde{x}_i(\tau T_i/T)\tilde{y}_i(\tau T_i/T - \lambda)}{\sqrt{\sum_{i=1}^{N} \tilde{x}_i(\tau T_i/T)^2}\sqrt{\sum_{i=1}^{N} \tilde{y}_i(\tau T_j/T - \lambda)^2}} \tag{2}$$

where $\tilde{x}_i(t)$ and, similarly, $\tilde{y}_i(t)$ were defined by

$$\tilde{x}_i(t) = x_i(t) - \sum_{i=1}^{N} x_i(t)/N \tag{3}$$

In this calculation, the SVS signal for each stride ($i = 1, \ldots, N$; $N = 380$) is denoted by $x_i(t)$, and the EMG signal for each stride ($i = 1, \ldots, N$) is described by $y_i(t)$. Here y_i can represent either the time domain EMG signal, or the wavelet coefficient at a particular frequency. The factor T_i/T adjusts for the different stride durations and ensures we are correlating quantities at the same phase in the stride. When computing the correlation, we interpolate signals x_i and y_i where necessary, as

$\tau T_i/T$ is not aligned with the sample times at which they were measured. Note that, in the case of the frequency domain analysis, C is also a function of frequency. Gain estimates H were defined as (31):

$$H_{(\lambda)} = \frac{\mathrm{CSD}(x, y)}{\mathrm{PSD}(x)} \quad (4)$$

where CSD(x,y) is the cross-spectral density of the SVS and EMG signals, and PSD(x) is the power spectral density of the SVS signal. Gain estimates were calculated for time frequency analysis similarly as the coherence estimates.

For illustrative purposes, time-dependent coherence and time-dependent cross-correlations were averaged between subjects to represent the global response from all subjects.

To validate the technique, two additional analyses were performed. First, we examined whether the amplitude of the time-dependent SVS-EMG coherence changed over the testing session. To do this, we determined the peak coherence for the first and last 100 steps of each subject and then compared these values using a paired t-test. Second, we determined the minimum number of steps required to obtain results that approximate the total 380 steps. To do this, coherence was estimated for increasing number of steps in 25-step increments (25, 50, 75, . . . 375). The difference in coherence between the 380-step total and each of the 25-step increments was determined by computing the normative error:

$$\text{error} = \sqrt{\sum \left(|C_{380}| - |C_n| \right)^2} \quad (5)$$

where C is the time-dependent coherence, and n is the lesser step total. The normative errors for all step counts between 25 and 375 steps were then compared using repeated-measures ANOVA. Since the normative error for the 380-step count is zero, it was not compared with the other step totals. The statistical analyses were, therefore, restricted to determining the highest step count that had statistically greater error than the 375-step count. The minimum steps required to provide results with error comparable to the 375-step count was determined as the step total, which was 25 steps larger than the step total that was statistically different from the 375-step count. Statistical significance was set at $\alpha = 0.05$.

Data reduction and statistical analysis. On a subject-by-subject basis, cross-correlation and coherence were determined to be significantly different from zero when values exceeded a 95% confidence limit using the methods described by Halliday et al. (16). Both the confidence limit for the coherence and confidence interval for the cross-correlation were based on the number of disjoint segments ($n = 447$) used in the spectral averaging (for further detail, see Ref. 9). The confidence interval values for the cross-correlations were then normalized by the product of the vector norms of the SVS and EMG signals, providing limits appropriately scaled for units of correlation (10).

Similar statistical analyses were used for the time-dependent coherence and cross-correlations (33). Confidence limits for time-dependent correlations (in both the frequency and time domains) were derived from the number of strides ($n = 380$) performed by each subject. However, because of the two-dimensional nature of these correlations, our simulations indicated that a 99% confidence limit represented better an α level of 0.05. The significance levels for the time-dependent coherence and cross-correlation were, respectively, 0.012 and 0.11 for individual subjects.

When significant, we extracted the timing of the peak time-dependent coherence, gain, and cross-correlation. To determine whether the modulation of the vestibular-evoked muscle responses occurred in parallel to EMG modulation during the stride cycle, we compared the timing of the peak time-dependent coherence, gain, and cross-correlations to the maximal EMG response during the locomotor cycle using paired t-tests. We also examined if modulation of the short- and medium-latency muscle responses occurred concurrently by comparing the peak muscle response occurring at a lag of 60 and 145 ms using a paired t-test. The level of significance was set at $\alpha = 0.05$.

RESULTS

Subjects maintained a repeatable locomotor pattern and did not lose balance, despite the presence of the vestibular stimulation. On average, stride duration was 2.24 ± 0.09 s, while left toe off, left heel strike, and right toe off occurred, respectively, at 15 ± 3, 50 ± 5, and 64 ± 6% of the stride cycle. All subjects exhibited well-defined correlations between the SVS and EMG signals in both the frequency and time domains (Fig. 1). Coupling between SVS and the gastrocnemius muscle activity exhibited significant coherence in the 0- to 20-Hz bandwidth for all subjects, with the largest averaged peak occurring at 8.7 ± 4.7 and 7.2 ± 3.2 Hz for the right and left medial gastrocnemius muscles, respectively. The cross-correlation between the SVS and EMG signals showed significant responses of opposite polarity between legs in all subjects. The early peak correlation between signals occurred at 59 ± 3 and 60 ± 3 ms and reached maximal amplitudes of 0.048 ± 0.021 and −0.047 ± 0.14 for the right and left medial gastrocnemius muscles, respectively. The medium-latency responses were of opposite polarity and occurred at a latency of 146 ± 8 and 144 ± 7 ms, reaching maximal amplitudes of −0.038 ± 0.020 and 0.039 ± 0.19, respectively, for the right and left medial gastrocnemius muscles. In most subjects, a

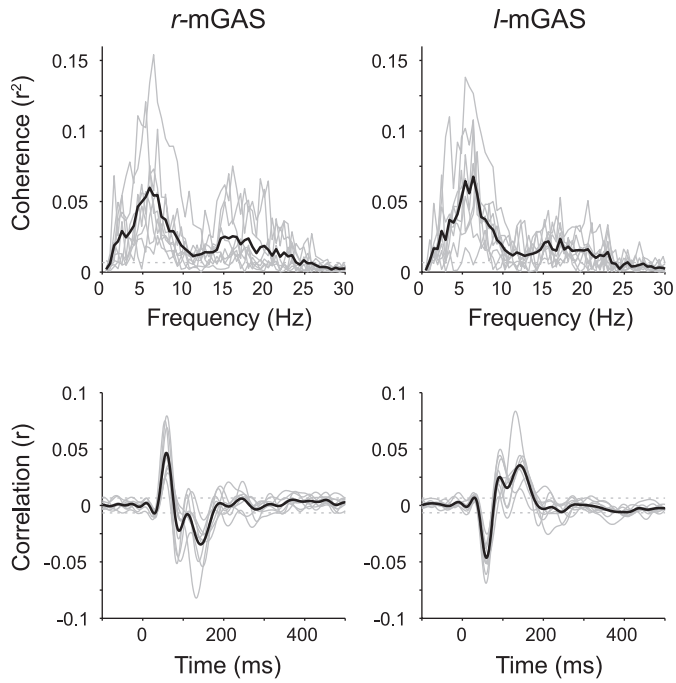

Fig. 1. Coherence and cross-correlations between stochastic vestibular stimulation (SVS) and medial gastrocnemius (mGas) muscles. *Top*: coherence between the SVS and EMG. *Bottom*: corresponding cross-correlations between these signals. The thick solid lines represent the average response from all subjects, and the thin shaded lines illustrate the individual responses from each subject. The horizontal dashed shaded lines show the confidence intervals computed for individual subject responses. For the coherence estimates, the confidence interval was 0.0067, whereas, for the cross-correlations, the confidence intervals were ±0.0066. Significant coherence was observed in all subjects in the 0- to 20-Hz bandwidth, and cross-correlations were significant around 50- and 150-ms lag, exhibiting opposite polarity between the left (l) and right (r) muscles.

small but significant intermediate response of the same polarity as the medium-latency response occurred between the short- and medium-latency responses (observed in seven of nine and eight of nine subjects, averaged amplitude -0.030 ± 0.019 and 0.029 ± 0.015 for the right and left medial gastrocnemius, respectively).

Time-dependent representations exhibited characteristic phasic modulation of SVS-EMG coherence for all subjects. The dynamic modulation of SVS-EMG coherence did not change over time, as peak coherence was similar between the first 100 steps and the last 100 steps (paired *t*-tests: $P > 0.05$; 0.27 ± 0.07 vs. 0.27 ± 0.13 and 0.24 ± 0.08 vs. 0.26 ± 0.1 for the right and left medial gastrocnemius, respectively). The minimum number of steps required to identify this modulation in single subjects was as few as 250 steps compared with 375 steps. This was demonstrated by the difference in time-dependent coherence observed at 225 steps for the left [$F_{(14,112)} = 106$, $P < 0.05$] and 250 steps for the right [$F_{(14,112)} = 176$, $P < 0.05$] medial gastrocnemius (Fig. 2).

Maximal time-dependent coherence was observed at 5.5 ± 0.8 and 5.2 ± 0.5 Hz, reaching amplitudes of 0.21 ± 0.11 and 0.22 ± 0.11 for the right and left medial gastrocnemius muscles, respectively (Fig. 3). Coherence increased during the stance phase of the stride cycle when the gastrocnemius muscles were active, reaching maximal values during the portion of single-leg support (21 ± 4 and $70 \pm 5\%$ of the stride cycle for the right and left medial gastrocnemius, respectively) (Fig. 3). Maximal coherence was observed before background EMG activity reached its peak (paired *t*-tests: $P < 0.001$; 21 ± 4 vs. $38 \pm 5\%$ and 70 ± 5 vs. $89 \pm 6\%$ of the stride cycle for the right and left medial gastrocnemius, respectively). Maximal SVS-EMG gain also peaked before background EMG activity reached its peak amplitude (paired *t*-tests: $P < 0.001$; 27 ± 3 vs. $38 \pm 5\%$ and 74 ± 3 vs. $89 \pm 6\%$ of the stride cycle for the right and left medial gastrocnemius, respectively). Minimal or no coherence was observed between SVS and EMG signals during the swing phase of the locomotor cycle.

The time-dependent cross-correlations between SVS and EMG signals exhibited clear phasic modulations of the biphasic muscle responses (Fig. 4). The polarity of the responses, however, remained constant throughout the stride cycle. Hence, when a response was visible in the left medial gastrocnemius (i.e., during stance phase), it exhibited a negative short-latency response, followed by a positive medium-latency response. Responses of opposite polarity were observed in the right medial gastrocnemius. The time-dependent cross-correlations between the SVS and muscle responses exhibited the largest correlation occurring during the rising phase of the background EMG signal. On average, the peak short-latency SVS-EMG cross-correlation occurred earlier than the peak background EMG signal (paired *t*-tests: $P < 0.001$; 23 ± 8 vs. $38 \pm 5\%$ and 71 ± 5 vs. $89 \pm 6\%$ of the stride cycle for the right and left medial gastrocnemius, respectively). On the other hand, the maximal SVS-EMG cross-correlation occurred at similar times for the short- and medium-latency responses (paired *t*-tests: $P > 0.5$; 23 ± 8 vs. $23 \pm 10\%$ and 71 ± 5 vs. $70 \pm 7\%$ of the stride cycle for the right and left medial gastrocnemius, respectively).

DISCUSSION

The aim of the present study was to determine whether time and frequency domain correlation techniques could be used to investigate human vestibular reflexes during locomotion. We hypothesized that, similar to felines, vestibular reflexes would be simultaneously modulated with extensor tone across the gait cycle, exhibiting their largest responses in correspondence with peak extensor muscle activity. Partly supporting our hypothesis, analysis of the SVS-EMG correlations as time-dependent processes permitted the identification of phase-dependent modulation of the vestibular reflexes during the stride cycle. As such, vestibular information from the stimulus exerts its influence over gastrocnemius muscle activity early in stance phase, eliciting a multiphasic muscle response. In contrast to our initial hypothesis, however, the period of maximal correlation between the vestibular stimulus and muscle activity did not correspond to the period of maximal EMG. These results demonstrate usefulness of this technique in extracting the modulation of vestibular reflexes over a cyclic task, such as locomotion.

Phase-dependent modulation of vestibular signals over the gait cycle has been documented in several species (17, 20–23, 27). These studies have suggested vestibular signals act to shape both the timing [in felines (29–30)] and magnitude [in guinea pigs (20–21)] of muscle activity during locomotion. In humans, phasic modulation of vestibular input to muscles has been directly observed only once, with limited resolution (17). Our results correspondingly demonstrate that vestibular input is indeed modulated with the phase of the gait cycle, and the period of vestibulomuscular coupling corresponds to the period of extensor muscle activation. There are, however, differences in the amplitude profile of the SVS-EMG coherence, gain, and

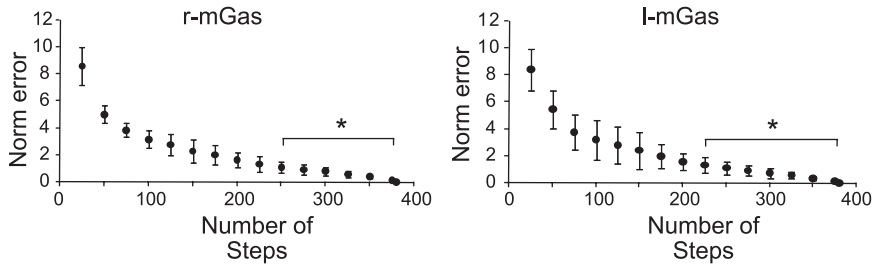

Fig. 2. Decrease in time-dependent coherence-related error associated with increasing the total steps in the average. These two graphs represent the error between the coherence for the full 380 steps and lesser step totals at 25-step increments (25, 50, 75, . . ., 375 steps) for both muscles plotted with their standard deviations. The error was defined by *Eq. 5*. Time-dependent coherence error estimated with step numbers <225–250 steps is significantly greater than the coherence error exhibited with 375 steps. Therefore, at least 250 steps are required to obtain a coherence difference error that is not different from that of the 375-step total. *Statistical significance.

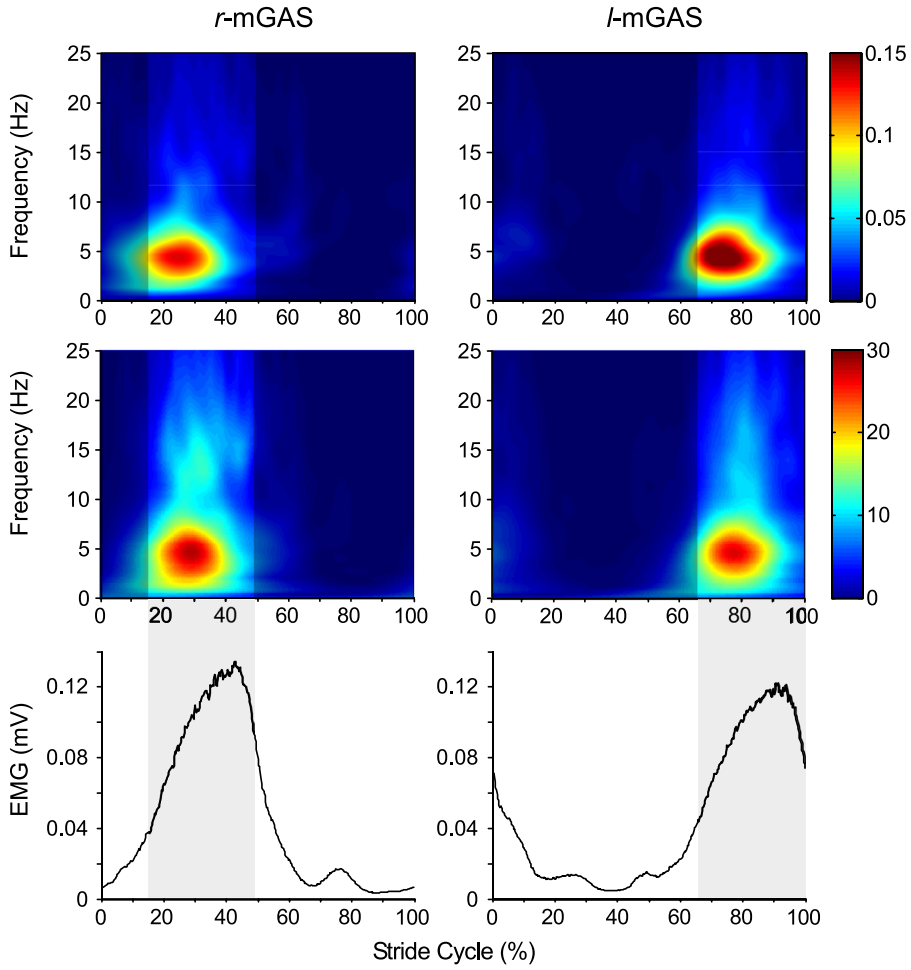

Fig. 3. Time-dependent SVS-EMG coherence and gain for the right and left mGas muscles. *Top*: averaged time-dependent coherence between the SVS and EMG (n = 9). *Middle*: the average time-dependent gain between the SVS and muscle signals (n = 9). *Bottom*: the modulation of the corresponding muscle during the stride cycle (n = 9). All figures are represented with *time 0* showing right heel strike. The color bar represents the amplitude of the coherence and gain, and the shaded area, the period of single-limb support for the right and left leg. Significant coherence and gain were observed during the period of stance phase of the stride cycle (i.e., while the corresponding ankle extensor was active), both of which reached maximal amplitude before background EMG reached its peak amplitude. Note that, for illustrative purposes, the time-frequency representations were shifted by 50 ms to account for the delay between SVS and muscle activation (see Fig. 1, *bottom*).

the gastrocnemius EMG over time. In the right gastrocnemius, for example, the increase in SVS-EMG coherence and gain initially parallels the rise in muscle activation peaking at 21 and 27% of the gait cycle, but then falling back to baseline levels at the 50% point of gait cycle. EMG, in contrast, continues to increase, reaching a maximum at the 38% point of the gait cycle. The discordance between SVS-EMG coupling and EMG amplitude indicates *1*) vestibular reflex amplitude is not purely dependent on the level of excitation of the motoneuron pool, and *2*) vestibular ex-afference does not appear to provide a large contribution to peak gastrocnemius muscle activation, instead contributing to the early rise in extensor activation. As well, the difference in timing between peak SVS-EMG coherence and peak EMG may be suggestive of the functional role of vestibular input to the gastrocnemius muscles during locomotion. Since the maximal influence of vestibular input to the gastrocnemius motoneurons was before maximal activation of the muscle, a potential role of the gastrocnemius to a vestibular error could be to stabilize the ankle before push-off. In addition, Bent et al. (1) have proposed that vestibular information plays an important role in whole body stabilization during locomotion and may influence foot placement. Our results may support this proposal as the high SVS-EMG coherence early in the single-support phase is appropriately timed to influence mediolateral placement of the contralateral foot.

The improved resolution of the technique presented here also allows a closer examination of vestibular reflex polarity across time. As seen in Figs. 1 and 4, vestibular stimulation during locomotion induces multiphasic muscle responses, reminiscent of those induced during standing balance (6, 18, 26). During standing balance, vestibular stimulation elicits a biphasic waveform, which has been described as containing a short- (50–70 ms) and medium-latency (100–120 ms) component (6, 9, 12, 18, 26). The waveform induced by vestibular stimulation during walking also appears to contain a short-latency component. The medium-latency component, however, appears more complex, exhibiting its own multiphasic waveform. During standing balance, the two components of the vestibular response have been described as being derived from independent spinal pathways (vestibule- and reticulospinal) (6), or originating from separate vestibular organelles (the otoliths or semicircular canals) (7). However, covariation in the amplitude of these two components observed during locomotion does not allow us to distinguish between these two processes.

The current approach provides several advantages over the more traditionally used GVS method when characterizing dynamically modulated responses in a cyclic task. First, changes in both the spatial and temporal parameters of the response can be observed as they occur in time. This is evident in both the strength of vestibulomuscular coupling over the gait cycle (Fig. 3), as well as the bilateral modulation of reflex polarity (Fig. 4).

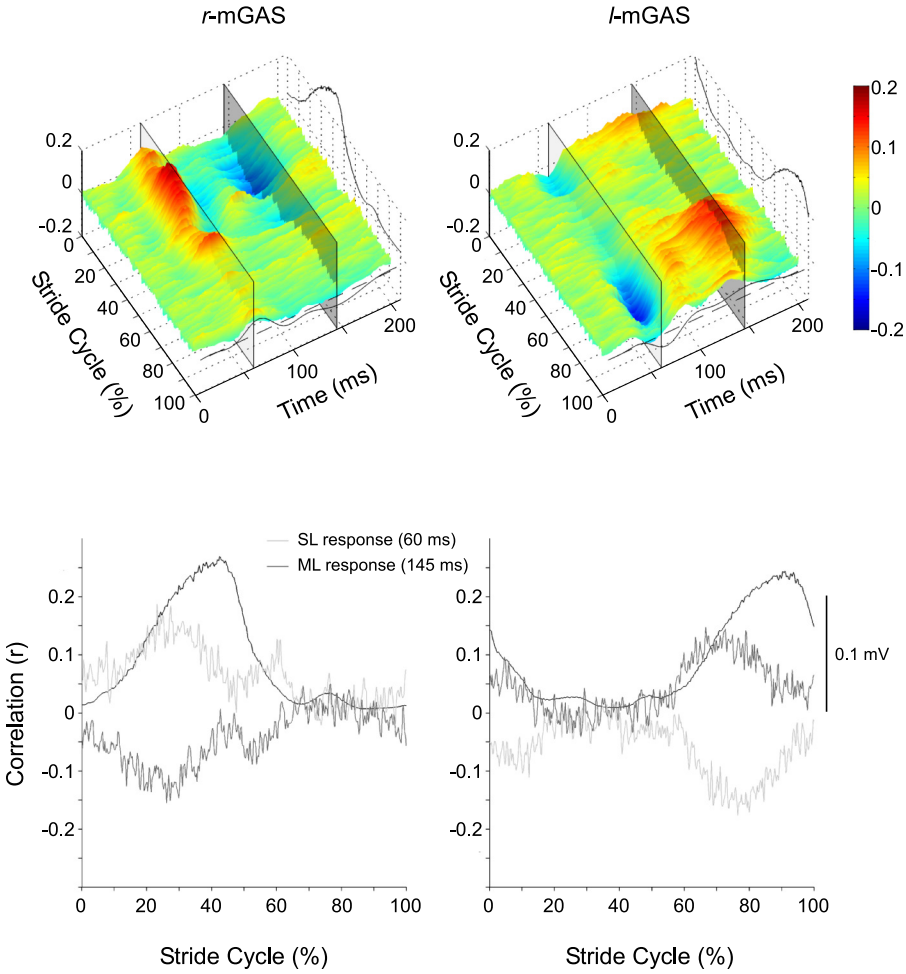

Fig. 4. Time-dependent cross-correlation between SVS-EMG for the right and left mGas muscles. *Top*: the averaged time-dependent cross-correlation between the SVS and EMG (n = 9). *Bottom*: the modulation of the short- (SL) and medium-latency (ML) responses during the stride cycle (n = 9). For the *top* panels, the black lines along the time (ms) axis represent the averaged cross-correlation for the stride cycle (see Fig. 1), while the black lines along the stride cycle (%) axis represent the modulation of muscle activity during the stride cycle. Maximal cross-correlations were observed during the stance phase of the stride cycle (i.e., while the corresponding ankle extensor was active), but reached maximal correlation before background EMG reached its peak amplitude. The transparent rectangles represent the time lags for which the SL (light gray) and ML (dark gray) response are represented for the *bottom* panels. The *bottom* panels illustrate the concurrent modulation of the SL and ML responses during the stride cycle. All figures are represented with *time 0* showing right heel strike. The color bar represents the amplitude of the cross-correlation. Note that, for illustrative purposes, the time-dependent cross-correlations were shifted by 50 ms to account for the delay between SVS and muscle activation.

Second, the continuous nature of the stimulus eliminates the need to time lock multiple stimuli to specific events in the task cycle, thus reducing testing time. Finally, the disruption of the locomotor pattern caused by the postural response to the stimulus can be reduced. In the present experiment, subjects maintained a stereotypical locomotor pattern and did not lose balance. In addition, it is possible to adjust the parameters of the SVS to minimize any balance disturbance while eliciting the proper vestibular responses in the muscles of interest (10). Since the largest balance responses to vestibular stimulation are associated with frequencies of stimulation below 2 Hz (10), and the bandwidth of significant coherence observed in the medial gastrocnemius begins at 2 Hz, these frequencies can be easily removed from the stimulus. There are, however, also some limitations to this technique.

One of the main limitations of the current approach is that, although phase-dependent modulation of human vestibular reflexes is revealed, the locus of such modulation cannot be identified. For the present results, it is not possible to determine whether the phasic modulation of vestibulomotor responses occurs due to inhibition of vestibular signals in the brain stem, inhibition by the cerebellum or due to modulation of the vestibulomotor action at the spinal level. Presently, the timing of vestibular influence over muscle activity is believed to be, in part, determined by activity arising from or passing through the cerebellum, as its removal, in felines, attenuates gait cycle-specific modulation (27). Presumably, inhibitory cerebellar Purkinje cells exert their influence over central vestibular neurons in the lateral vestibular nucleus, resulting in the phase-dependent behavior of vestibulomuscle interactions during gait (19, 32).

In addition, the description of SVS-evoked vestibular activity itself as an ex-afferent signal may also present limitations. Most sensory disturbances that create an ex-afferent signal also exhibit congruent input from multiple sensory modalities. With SVS, the vestibular response is incongruent with both visual and somatosensory inputs and, therefore, may be interpreted by the body in a manner different than had the vestibular input been in congruence with visual and somatosensory inputs. Controlling locomotor speed by using a treadmill may present some further limitations. By constraining locomotor speed, participants were required to walk at cadences that differed in various amounts from their natural cadence. These parameters were chosen to match those used in previous experiments (13, 15, 17); however, the slower than preferred locomotor speed likely resulted in alterations in participant's gait mechanics, as well as alterations in the balance requirements of the task.

Our final limitation relates to the limited analyses presented here. For the sake of brevity, analyses have been limited to a single muscle (bilaterally) and only for roll balance perturbations. Outside of the lower leg, the distribution and influence of vestibular signals on lower limb motor control is still unknown.

Future work needs to focus these techniques on examining widespread vestibular contributions to dynamic muscle activity in humans.

Conclusions. The results of the present study demonstrate that time and frequency domain correlation techniques can be used to investigate human vestibular reflexes during locomotion and provide a basic framework for extracting reflex modulation to continuous randomly varying stimuli. This approach was effective in extracting the phase-dependent modulation of vestibulomuscular coupling during a cyclic task, revealing that the period of strongest vestibulomuscular coupling occurred during single-leg support before the period of maximal EMG activity in the gastrocnemius. Together, these findings suggest a functional role of the gastrocnemius muscle to a vestibular error before the push-off phase of locomotion.

ACKNOWLEDGMENTS

We thank Tammy Law for help with data processing and Melanie Roskell for contribution in collecting pilot data.

GRANTS

This study was funded by the Natural Sciences and Engineering Research Council of Canada. J.-S. Blouin received salary support from the Canadian Institutes of Health Research-Canadian Chiropractic Research. Foundation and Michael Smith Foundation for Health Research. K. van den Doel was supported by the Peter Wall Institute's Major Thematic Grant on Sensorimotor Computation.

DISCLOSURES

No conflicts of interest, financial or otherwise, are declared by the author(s).

REFERENCES

1. **Bent LR, Inglis JT, McFadyen BJ.** When is vestibular information important during walking? *J Neurophysiol* 92: 1269–1275, 2004.
2. **Bent LR, McFadyen BJ, Merkley VF, Kennedy PM, Inglis JT.** Magnitude effects of galvanic vestibular stimulation on the trajectory of human gait. *Neurosci Lett* 279: 157–160, 2000.
3. **Borel L, Harley F, Lopez C, Magnan J, Chays A, Lacour M.** Walking performance of vestibular-defective patients before and after unilateral vestibular neurotomy. *Behav Brain Res* 150: 191–200, 2004.
4. **Brandt T.** Vestibulopathic gait: you're better off running than walking. *Curr Opin Neurol* 13: 3–5, 2000.
5. **Brillinger DR.** Cross-spectral analysis of processes with stationary increments including the stationary Queue. *Ann Probab* 2: 815–827, 1974.
6. **Britton TC, Day BL, Brown P, Rothwell JC, Thompson PD, Marsden CD.** Postural electromyographic responses in the arm and leg following galvanic vestibular stimulation in man. *Exp Brain Res* 94: 143–151, 1993.
7. **Cathers I, Day BL, Fitzpatrick RC.** Otolith and canal reflexes in human standing. *J Physiol* 563: 229–234, 2005.
8. **Dakin CJ, Inglis JT, Blouin JS.** Short and medium latency muscle responses evoked by electrical vestibular stimulation are a composite of all stimulus frequencies. *Exp Brain Res* 209: 345–354, 2011.
9. **Dakin CJ, Lee Son GM, Inglis JT, Blouin JS.** Frequency response of human vestibular reflexes characterized by stochastic stimuli. *J Physiol* 583: 1117–1127, 2007.
10. **Dakin CJ, Luu BL, van den Doel K, Inglis JT, Blouin JS.** Frequency-specific modulation of vestibular-evoked sway responses in humans. *J Neurophysiol* 103: 1048–1056, 2010.
11. **Day BL, Fitzpatrick RC.** Virtual head rotation reveals a process of route reconstruction from human vestibular signals. *J Physiol* 567: 591–597, 2005.
12. **Fitzpatrick R, Burke D, Gandevia SC.** Task-dependent reflex responses and movement illusions evoked by galvanic vestibular stimulation in standing humans. *J Physiol* 478: 363–372, 1994.
13. **Fitzpatrick RC, Butler JE, Day BL.** Resolving head rotation for human bipedalism. *Curr Biol* 16: 1509–1514, 2006.
14. **Fitzpatrick RC, Day BL.** Probing the human vestibular system with galvanic stimulation. *J Appl Physiol* 96: 2301–2316, 2004.
15. **Fitzpatrick RC, Wardman DL, Taylor JL.** Effects of galvanic vestibular stimulation during human walking. *J Physiol* 517: 931–939, 1999.
16. **Halliday DM, Rosenberg JR, Amjad AM, Breeze P, Conway BA, Farmer SF.** A framework for the analysis of mixed time series/point process data-theory and application to the study of physiological tremor, single motor unit discharges and electromyograms. *Prog Biophys Mol Biol* 64: 237–278, 1995.
17. **Iles JF, Baderin R, Tanner R, Simon A.** Human standing and walking: comparison of the effects of stimulation of the vestibular system. *Exp Brain Res* 178: 151–166, 2007.
18. **Iles JF, Pisini JV.** Vestibular-evoked postural reactions in man and modulation of transmission in spinal reflex pathways. *J Physiol* 455: 407–424, 1992.
19. **Ito M, Yoshida M.** The cerebellar evoked monosynaptic inhibition of deiters' neurons. *Experientia* 20: 515–516, 1964.
20. **Marlinsky VV.** Activity of lateral vestibular nucleus neurons during locomotion in the decerebrate Guinea pigs. *Exp Brain Res* 90: 583–588, 1992.
21. **Marlinsky VV.** The influence of adequate vestibular stimulation on evoked locomotor muscle activity in the decerebrated guinea-pig. *Neuroscience* 33: 643–650, 1989.
22. **Matsuyama K, Drew T.** Vestibulospinal and reticulospinal neuronal activity during locomotion in the intact cat. I. Walking on a level surface. *J Neurophysiol* 84: 2237–2256, 2000.
23. **Matsuyama K, Drew T.** Vestibulospinal and reticulospinal neuronal activity during locomotion in the intact cat. II. Walking on an inclined plane. *J Neurophysiol* 84: 2257–2276, 2000.
24. **Mian OS, Dakin CJ, Blouin JS, Fitzpatrick RC, Day BL.** Lack of otolith involvement in balance responses evoked by mastoidal stimulation. *J Physiol* 588: 4441–4451, 2010.
25. **Misiaszek JE.** Neural control of walking balance: if falling then react else continue. *Exerc Sport Sci Rev* 34: 128–134, 2006.
26. **Nashner LM, Wolfson P.** Influence of head position and proprioceptive cues on short latency postural reflexes evoked by galvanic stimulation of the human labyrinth. *Brain Res* 67: 255–268, 1974.
27. **Orlovsky GN.** Activity of vestibulospinal neurons during locomotion. *Brain Res* 46: 85–98, 1972.
28. **Rosenberg JR, Amjad AM, Breeze P, Brillinger DR, Halliday DM.** The fourier approach to the identification of functional coupling between neuronal spike trains. *Prog Biophys Mol Biol* 53: 1–31, 1989.
29. **Russell DF, Zajac FE.** Effects of stimulating Deiters' nucleus and medial longitudinal fasciculus on the timing of the fictive locomotor rhythm induced in cats by DOPA. *Brain Res* 177: 588–592, 1979.
30. **Udo W, Kamei H, Matsukawa K, Tanaka K.** Interlimb coordination in cat locomotion investigated with perturbation. *Exp Brain Res* 46: 438–447, 1982.
31. **van der Kooij H, van Asseldonk E, van der Helm FCT.** Comparison of different methods to identify and quantify balance control. *J Neurosci Methods* 145: 175–203, 2005.
32. **Walberg F, Jansen I.** Cerebellar corticovestibular fibers in the cat. *Exp Neurol* 3: 32–52, 1961.
33. **Zhan Y, Halliday DM, Jiang P, Liu X, Feng J.** Detecting time-dependent coherence between non-stationary electrophysiological signals. A combined statistical and time-frequency approach. *J Neurosci Methods* 156: 322–332, 2006.